

Supplemental Figure Legends to NR2F1 underlies the persistence of 'invasive-state' residual disease after treatment of *BRAF*-mutant melanoma.

Supplemental Figure S1. NR2F1 expression in melanoma. (A) Statistical analysis of NR2F1 expression from Fig. 1A. **(B)** Normalized expression of NR2F1 for dynamic transcriptome cell states and **(C)** normalized expression of NR2F1 for MAPKi-resistant cell states from Song/Hugo/Lo et al. 2017 (1), all in *BRAF*-mutant cell lines. **(D)** NR2F1 basal expression in *BRAF*-mutant, *NRAS*-mutant, and WT *BRAF* /WT *NRAS* melanoma cell line panel. WM1366TR-NR2F1+ was used as a positive control for NR2F1 expression. **(E)** Raw images used to quantify the expression of NR2F1 in minimal residual disease (MRD) from Fig. 1E. Magnification: 15X. **(F)** mRNA expression of NR2F1 in A375, CRT34, and CRT35 from GSE180568. **(G)** Western blot for NR2F1 expression in A375, CRT34, and CRT35 treated with or without BRAFi + MEKi for 24 hours (HSP90 as loading control). Quantification of band densitometry (NR2F1:HSP90 normalized to A375 without BRAFi + MEKi) is displayed under each band.

Supplemental Figure S2. Controls and assay quantifications for Figure 2. (A) Beta-galactosidase protein levels for the human *BRAF*-mutant melanoma cell line control, 1205LuTR-LacZ after 72 hours of treatment using BRAFi + MEKi + DOX (PLX4720 1 μ mol/L + PD0325901 35 nmol/L + doxycycline 100 ng/mL). Vinculin was used as a loading control. **(B)** RNA-seq reads for NR2F family member (NR2F1, NR2F2, long noncoding RNA NR2F1-AS1, long noncoding RNA NR2F2-AS1, and NR2F6) expression levels for NR2F1-expressing cell lines, 1205LuTR-NR2F1 (1205Lu), A375TR-NR2F1 (A375), and WM793TR-NR2F1 (WM793) after 72 hours of treatment using BRAFi + MEKi + DOX (PLX4720 1 μ mol/L + PD0325901 35 nmol/L + doxycycline 100 ng/mL). **(C)** Bar graph of colony formation assay results by percentage of the area covered by adherent cells. The bars represent the normalized values to DMSO groups. The data are shown as the mean \pm SEM with * p <0.05, ** p <0.01 and **** p <0.0001. **(D)** Spheroid outgrowth invasion

area quantification from Fig. 2D. Unpaired t-test *p<0.05 and **p<0.01.

Supplemental Figure S3. GSEA hallmark enrichment plots for NR2F1-overexpressing melanoma cells. (A) GSEA hallmark enrichment plots for MYC1 targets variant 2; (B) estrogen late response genes; (C) MYC1 targets variant 1, DNA repair, E2F targets, G2/M checkpoint, mitotic spindle, spermatogenesis; (D) cholesterol homeostasis, unfolded protein response, interferon-alpha response, interferon-gamma response, hypoxia; and (E) adipogenesis comparing NR2F1 expression (DOX) to no DOX after 72 hours of treatment using BRAFi + MEKi + DOX (PLX4720 1 µmol/L + PD0325901 35 nmol/L + doxycycline 100 ng/mL) in melanoma cells with inducible NR2F1 overexpression. (F) Heatmaps showing fold change values for altered genes in Dormancy Up and Down gene sets from Kim et al. (2). (G) Heatmap showing fold change values for altered dormancy related genes from Fane et al. (3). (H) Heatmap showing fold change values of REACTOME Cellular Senescence pathway genes that were significantly altered in at least one comparison. (I) Enrichment plots for KEGG cell cycle gene set. (J) Heatmap showing fold change values of genes from KEGG cell cycle gene set that were significantly altered in at least one comparison.

Supplemental Figure S4. MAPK and cell-cycle targets in NR2F1-overexpressing melanoma cells. (A) Western blot for cell survival-related proteins in NR2F1-overexpressing cells after 72-hour treatment with BRAFi + MEKi + DOX (PLX4720 1 µmol/L + PD0325901 35 nmol/L + doxycycline 100 ng/mL). Vinculin was used as a loading control. Please note that the NR2F1 blot is the same here and in Figure 4D. (B) Venn diagram of the 21 significantly overlapping mTORC1-related genes modulated by NR2F1 overexpression during BRAFi + MEKi therapy, taken from RNA-seq, in A375-NR2F1, 1205Lu-NR2F1, and WM793-NR2F1.

Supplemental Figure S5. Targeting mTORC1 in NR2F1-overexpressing melanoma. (A)

Western blot for phospho-S6 levels in NR2F1-overexpressing cells after 72-hour treatment with BRAFi (PLX4720 $\mu\text{mol/L}$) + MEKi (PD0325901 35 nmol/L) + AZD2014 (1 $\mu\text{mol/L}$) + DOX (doxycycline 100 ng/mL). Vinculin was used as a loading control. **(B)** 1205Lu xenograft mice weight loss for BRAFi + MEKi chow (PLX4720 200 ppm + PD0325901 7 ppm) +/- AZD2014 (20 mg/kg) treatment groups. AZD2014 was administered by oral gavage bi-daily for 2 days on/5 days off. **(C)** Raw images used to quantify the expression of NR2F1 in MRD from Fig. 5C. Magnification: 15X. **(D)** Weight of mice treated with BRAFi + MEKi + rapamycin from Fig. 5D-E.

Supplemental Figure S6. NR2F1 expression in aged BRAF-mutant melanoma models. (A)

Western blot for NR2F1 protein expression in YUMM1.7 allografts from young and aged mice. **(B)** Raw images used to quantify the expression of NR2F1 from Fig. 6B. Low Magnification (Mag.): 4X. High Mag.: 40X.

Supplemental Figure S7. Structures for inhibitors used in this manuscript. Source:

<https://pubchem.ncbi.nlm.nih.gov/>

Supplemental References

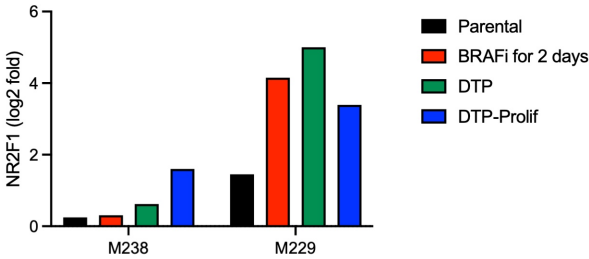
1. Song C, Piva M, Sun L, Hong A, Moriceau G, Kong X, et al. Recurrent tumor cell-intrinsic and -extrinsic alterations during MAPKi-induced melanoma regression and early adaptation. *Cancer Disc.* 2017;CD-17-0401.
2. Kim RS, Avivar-Valderas A, Estrada Y, Bragado P, Sosa MS, Aguirre-Ghiso JA, Segall JE. Dormancy signatures and metastasis in estrogen receptor positive and negative breast cancer. *PLoS One.* 2012;7(4):e35569.
3. Fane ME, Chhabra Y, Alicea GM, Maranto DA, Douglass SM, Webster MR, et al. Stromal changes in the aged lung induce an emergence from melanoma dormancy. *Nature.* 2022;606(7913):396-405.

A

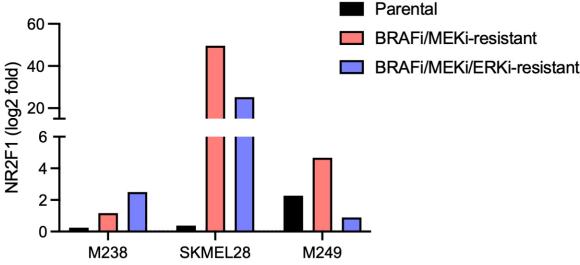
Statistical analysis for Fig 1A:

gene_ID	gene_name	avg_log2FC	p_val	p_val_adj	CellType_numerator	CellType_denominator
ENSG00000175745	NR2F1	3.91E-01	2.14E-05	8.01E-01	invasive	pigmented
ENSG00000175745	NR2F1	3.91E-01	2.14E-05	1.53E-01	invasive	immune
ENSG00000175745	NR2F1	3.91E-01	4.79E-07	1.79E-02	invasive	NCSC
ENSG00000175745	NR2F1	3.90E-01	1.61E-12	6.05E-08	invasive	proliferative
ENSG00000175745	NR2F1	3.86E-01	2.28E-17	8.54E-13	invasive	other
ENSG00000175745	NR2F1	3.87E-01	2.58E-24	9.67E-20	invasive	SMC

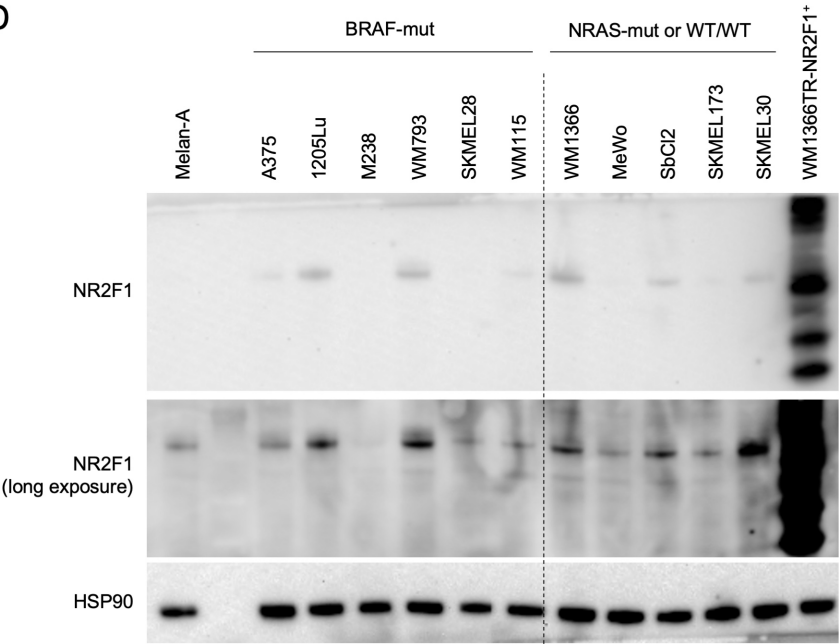
B



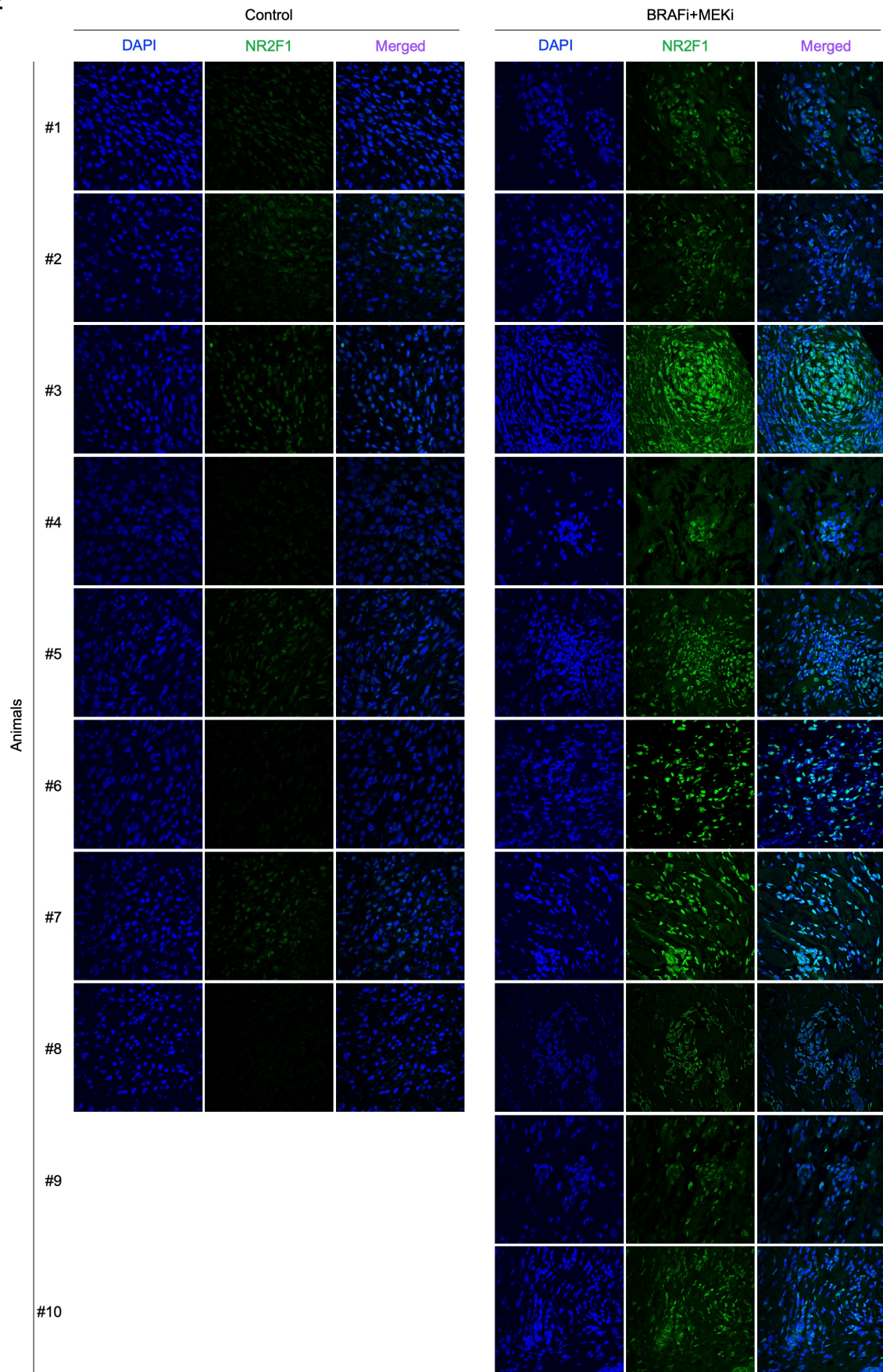
C



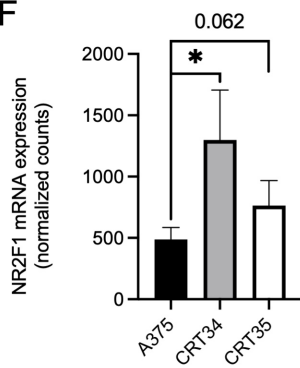
D



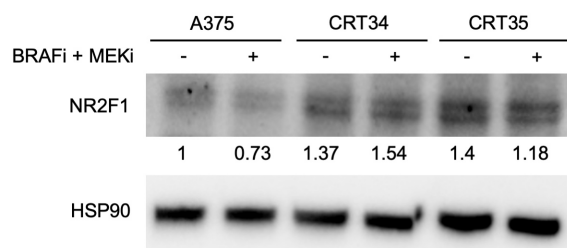
E

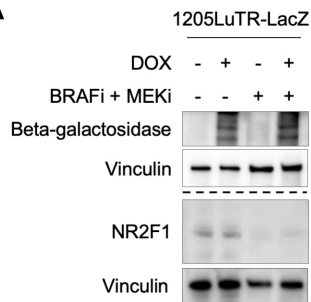
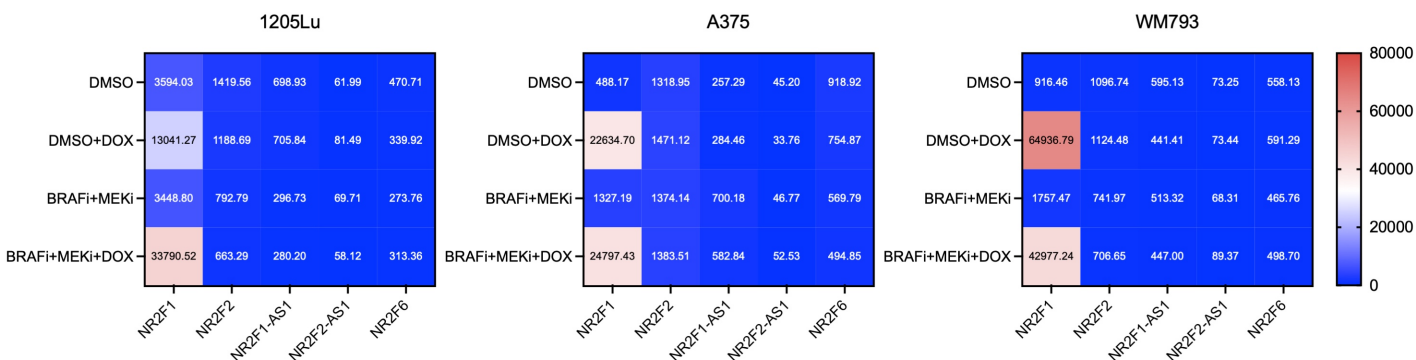
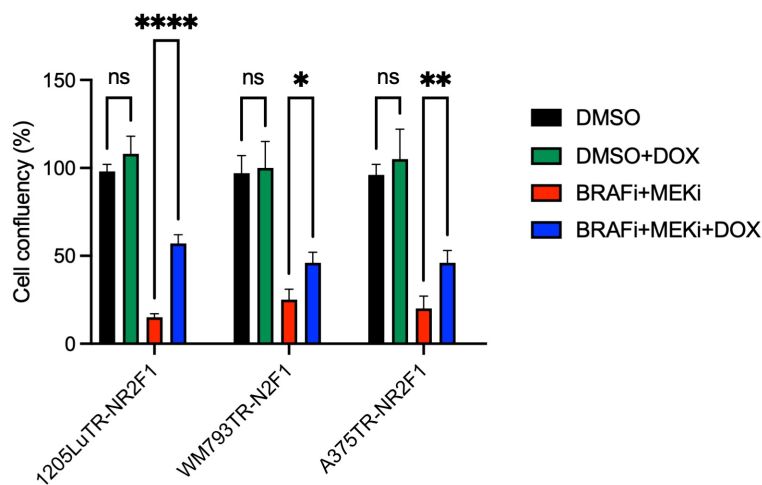
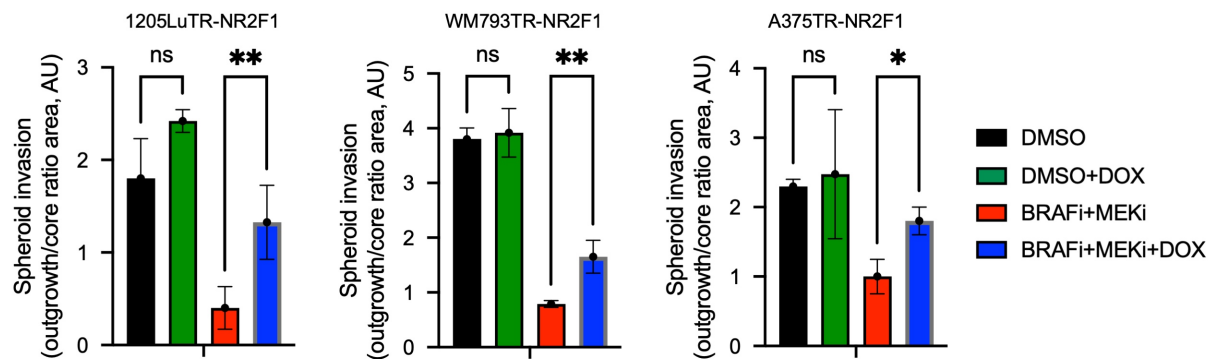


F



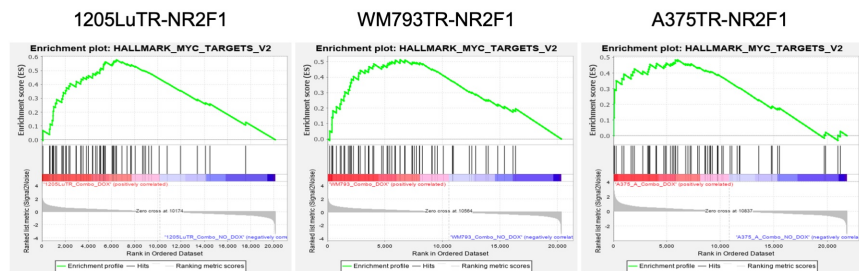
G



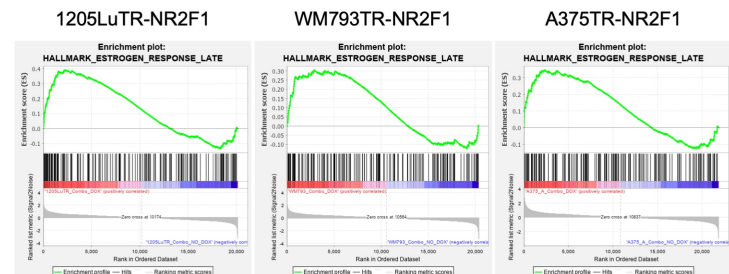
A**B**RNA-seq (reads) – NR2F proteins expression following BRAFi +MEKi (72h) *in vitro***C****D**

A

MYC targets V2



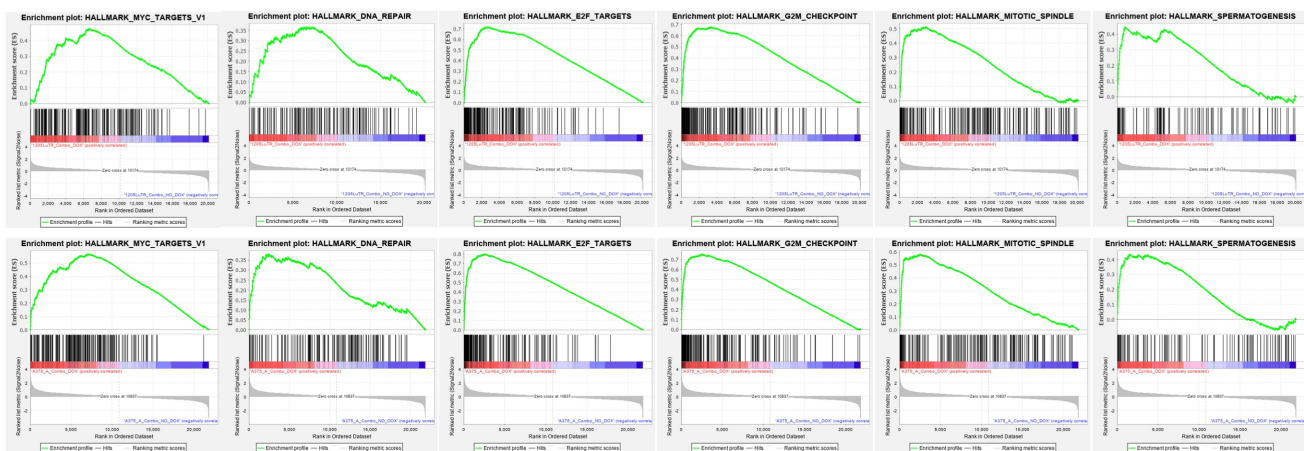
B



C

1205LuTR-NR2F1

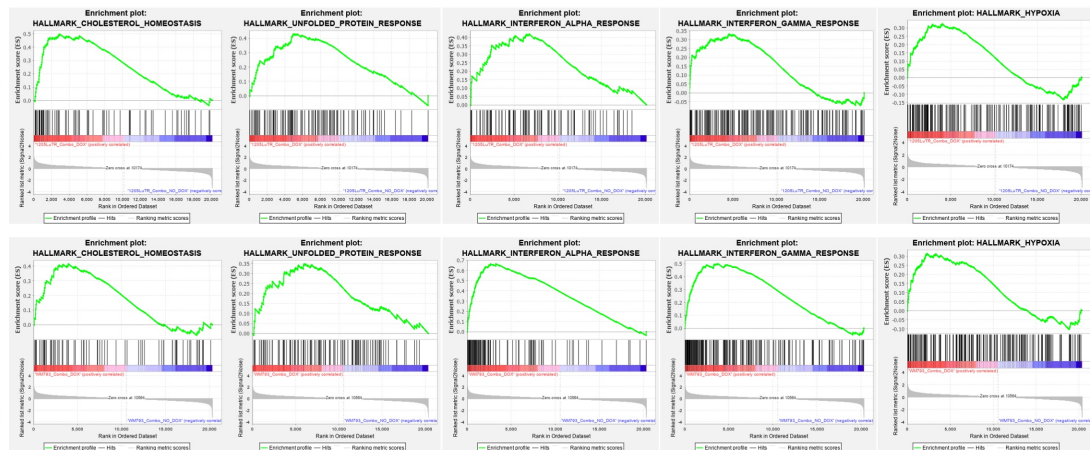
A375TR-NR2F1



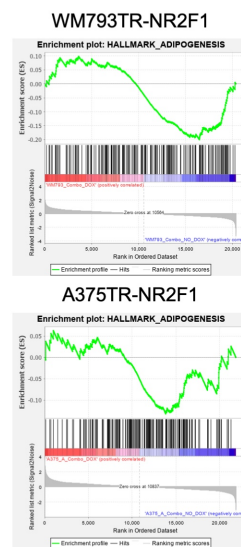
D

1205LuTR-NR2F1

WM793TR-NR2F1



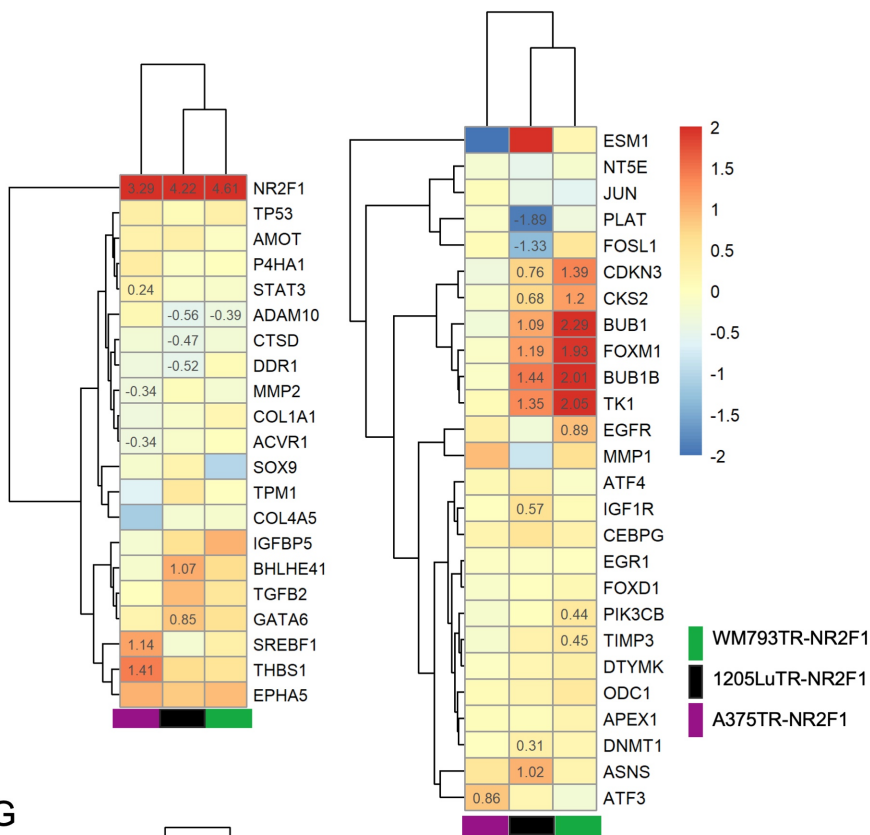
E



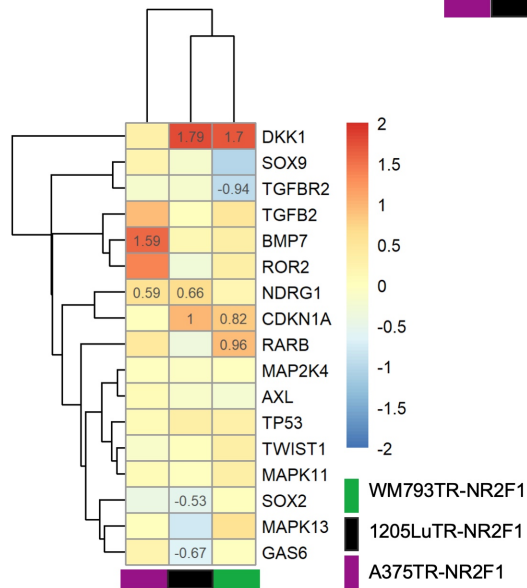
F

Dormancy Up

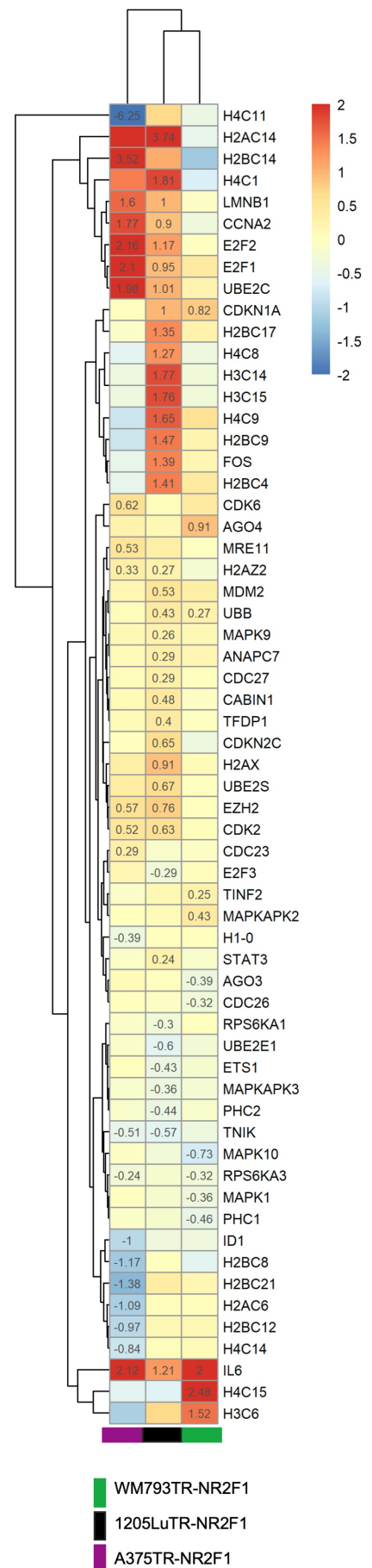
Dormancy Down



G



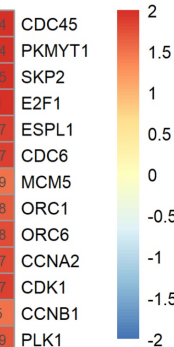
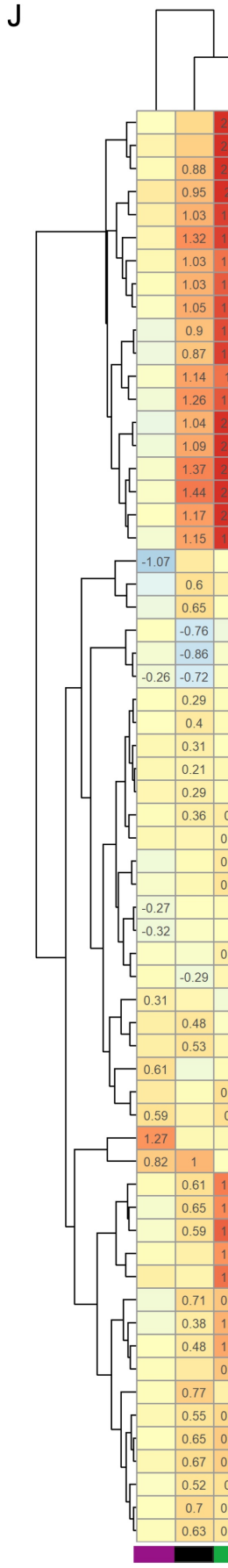
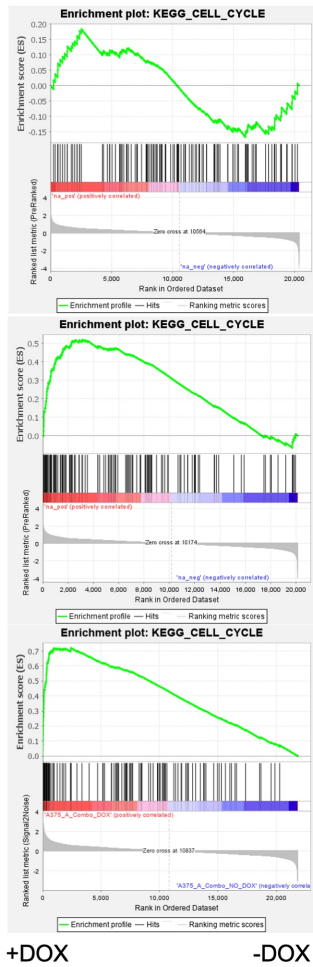
H



WM793TR
-NR2F1

1205LuTR
-NR2F1

A375TR
-NR2F1



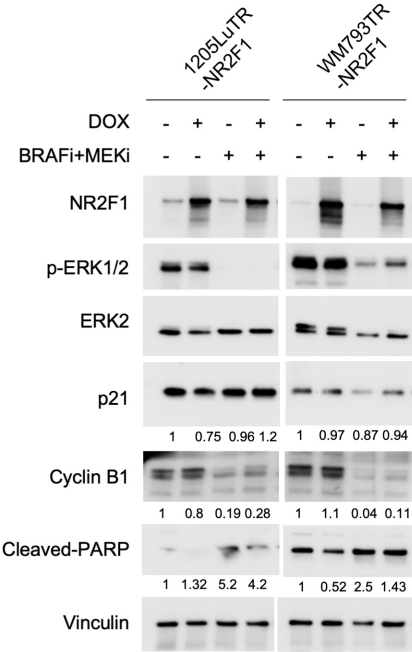
2.41	CDC45
2.24	PKMYT1
0.88	SKP2
0.95	E2F1
1.03	ESPL1
1.32	CDC6
1.03	MCM5
1.03	ORC1
1.05	ORC6
0.9	CCNA2
0.87	CDK1
1.14	CCNB1
1.26	PLK1
1.04	CDC25C
1.09	BUB1
1.37	CDC20
1.44	BUB1B
1.17	E2F2
1.15	CCNB2
-1.07	SMC1B
0.6	CDC7
0.65	CDKN2C
-0.76	TGFB1
-0.86	CDC14B
-0.26	HDAC1
0.29	CDC27
0.4	TFDP1
0.31	MAD2L2
0.21	BUB3
0.29	ANAPC7
0.36	PCNA
0.24	HDAC2
0.47	ORC3
0.55	SMAD3
-0.27	RBL2
-0.32	CDC26
0.29	CDC23
-0.29	E2F3
0.31	CCND3
0.48	CREBBP
0.53	MDM2
0.61	MAD1L1
0.62	CDK6
0.59	MYC
1.27	GADD45A
0.82	CDKN1A
0.61	MCM2
0.65	MCM4
0.59	MAD2L1
1.25	MCM6
1.48	CDC25A
0.71	PTTG1
0.38	CHEK2
0.48	CHEK1
0.87	WEE1
0.77	SMC1A
0.55	CDC25B
0.65	MCM3
0.67	MCM7
0.52	RBL1
0.7	DBF4
0.63	CDK2

WM793TR-NR2F1

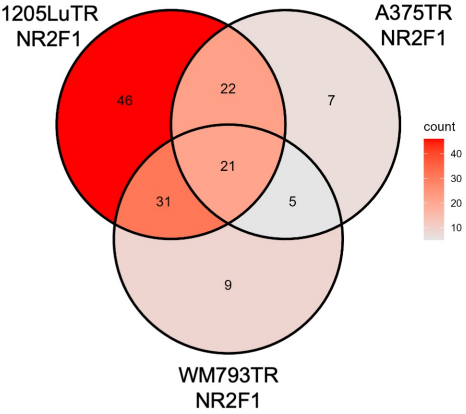
1205LuTR-NR2F1

A375TR-NR2F1

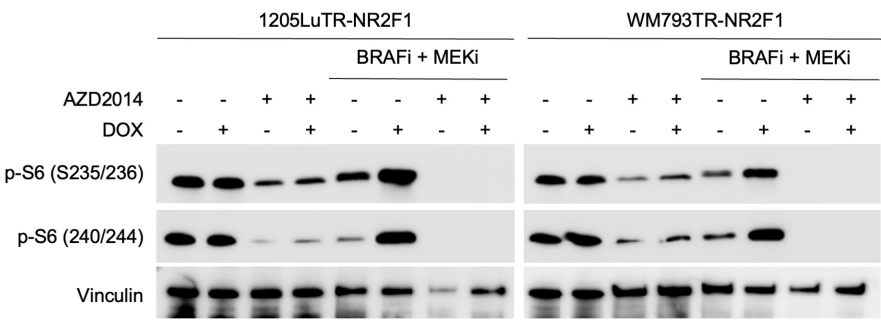
A



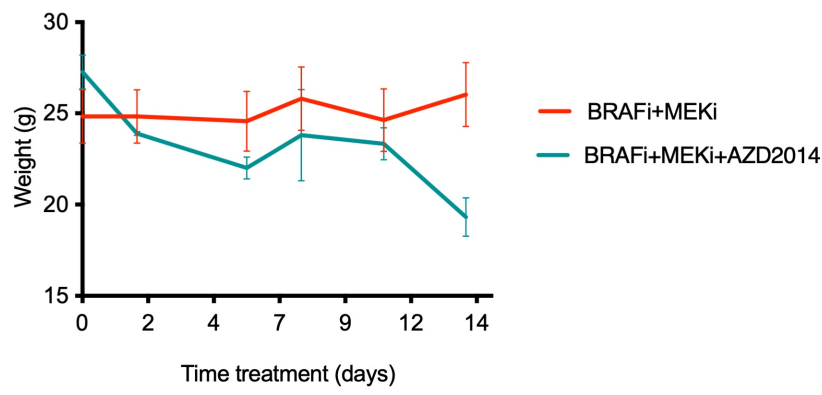
B



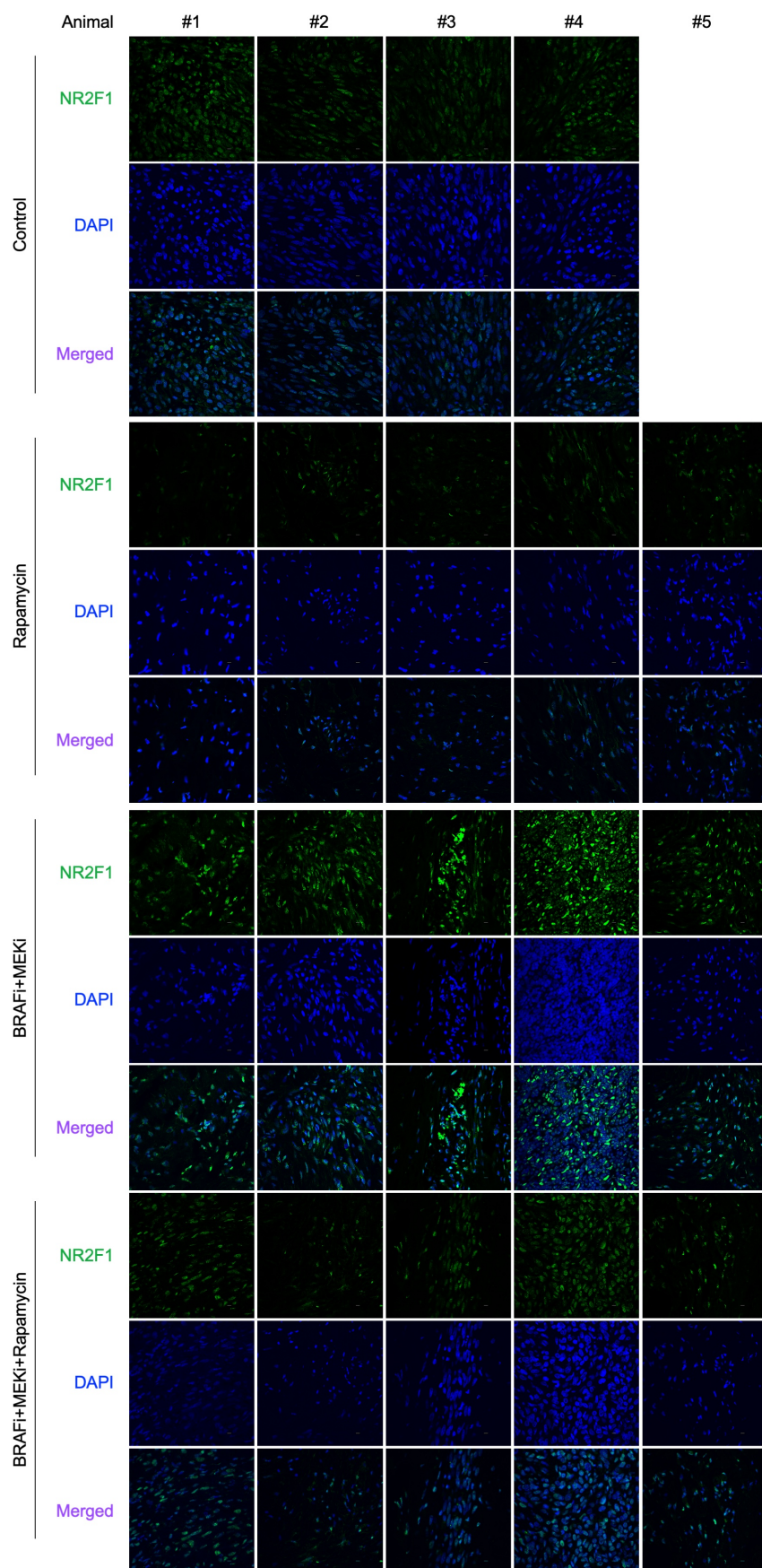
A

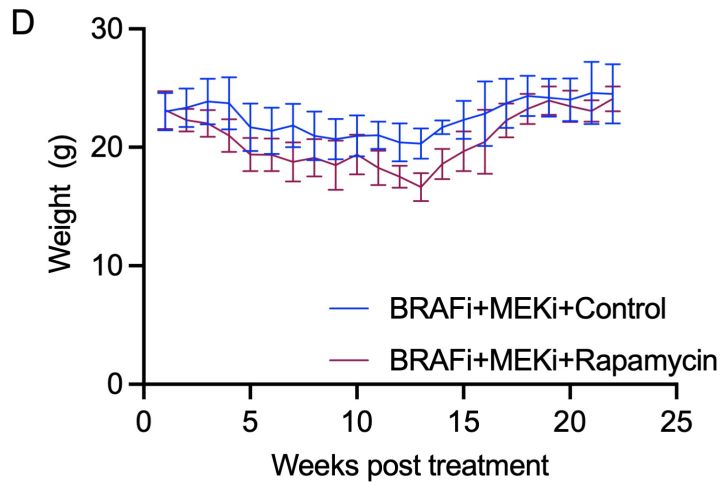


B

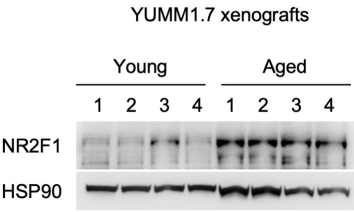


C

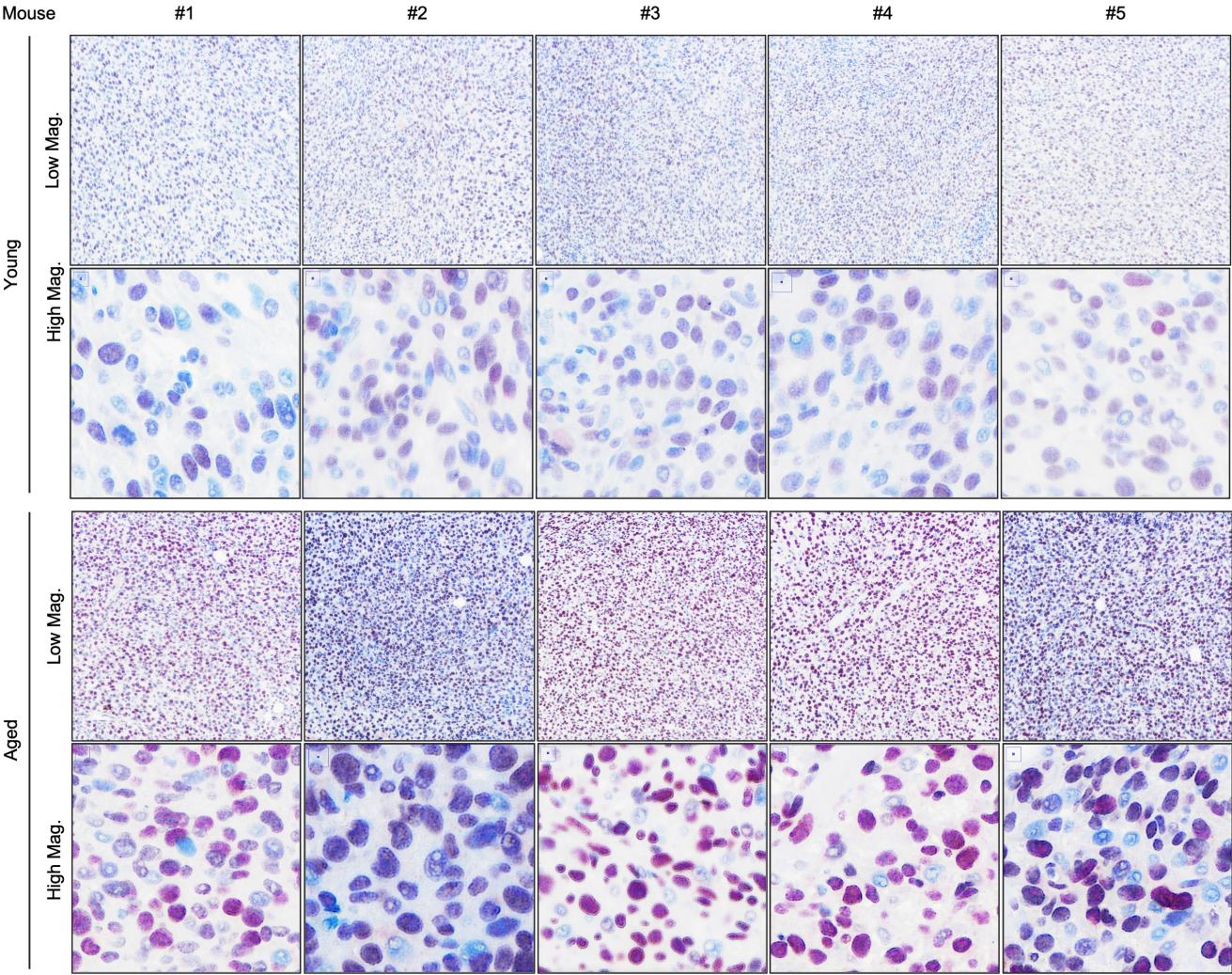




A

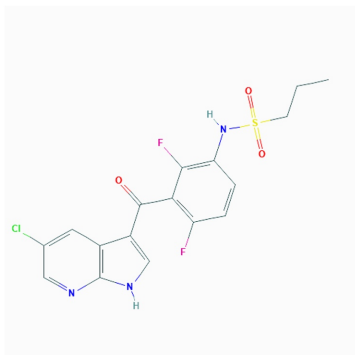


B



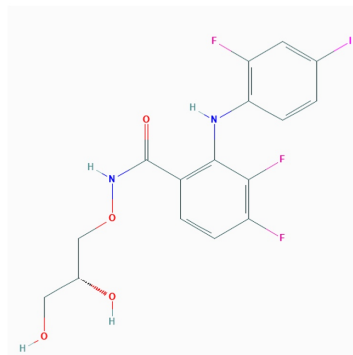
Chemical structures for agents used in this manuscript:

PLX4720



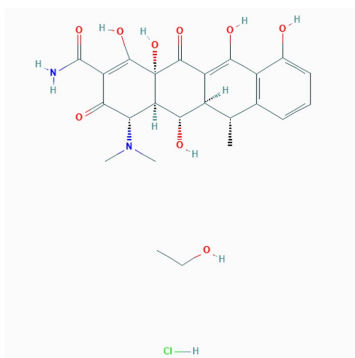
Molecular Formula:
C₁₇H₁₄ClF₂N₃O₃S

PD0325901



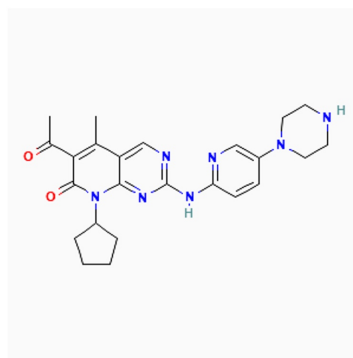
Molecular Formula:
C₁₆H₁₄F₃IN₂O₄

Doxycycline Hyclate



Molecular Formula:
C₂₄H₃₁ClN₂O₉

PD0332991



Molecular Formula:
C₂₄H₂₉N₇O₉